Check for updates

Endoscopic Transanterior Middle Temporal Approach to the Atrium—An Anatomical Feasibility Study

Ruth Lau[1,3], Roberto Rodriguez Rubio[1,2], Juan Martino[4], José L. Sanmillán[3], Arnau Benet[1,2,5], Ali Tayebi Meybodi[1,2,5], Sirin Gandhi[1,2,5], Ioannis Kournoutas[1], Andreu Gabarrós[3]

■ OBJECTIVE: **The atrium is the most common location for masses in the lateral ventricle. However, access to this area is limited owing to its deep location and adjacent eloquent neurovascular structures, such as the choroidal arteries, perisylvian white matter (WM) tracts, and optic radiations. We investigated the feasibility and safety of an endoscopic approach to the atrium via the anterior middle temporal gyrus (MTG).**

■ METHODS: **Radiological assessment of a minimally invasive surgical trajectory to the atrium was achieved in 10 patients. Surgical simulation to assess the feasibility of our endoscopic approach was performed on 24 cadaveric specimens using a transzygomatic corridor and temporal craniotomy. Preoperative computed tomography was performed to confirm the surgical trajectory using neuronavigation. Using Klinger's method, 5 hemispheres were dissected to assess the relationship of our approach to the WM tracts.**

■ RESULTS: **The optimal entry angle to reach the atrium through the anterior MTG was related to the temporal horn in the axial plane and to the Sylvian fissure in the sagittal plane. Our entry point in the anterior MTG was 19 ± 1.92 mm from the temporal pole. The transparenchymal distance to atrium was 24.55 ± 4.3 mm. The WM dissections confirmed that our approach did not violate the optic radiations, uncinate fasciculus, inferior fronto-occipital fasciculus, inferior longitudinal fasciculus, or superior longitudinal fasciculus.**

■ CONCLUSION: **Our findings have confirmed the feasibility of an anterior endoscopic approach to the atrium through the anterior MTG, with preservation of the functional integrity of the eloquent cortex and WM tracts.**

INTRODUCTION

The atrium is the most common location for lateral ventricular masses.[1] The largest series of intraventricular tumors reported a prevalence of intraventricular meningiomas of 0.5%–3% of all meningiomas, most commonly arising from the ventricular atrium (Figure 1).[2-4] Other atrial lesions include choroid plexus tumors[1,5-8] and cavernous angiomas.[9] The surgical approach to lesions located in the atrium is challenging. The difficulty starts with selection of the approach itself, owing to the target's deep location, the presence of

Key words
- Anterior middle temporal
- Atrium
- Choroidal arteries
- Endoscope
- Meyer's loop
- Optic radiations
- Perisylvian network
- Surgical approach

Abbreviations and Acronyms
CT: Computed tomography
ETMTA: Endoscopic transanterior middle temporal approach
ICP: Inferior choroidal point
IFOF: Inferior fronto-occipital fasciculus
ILF: Inferior longitudinal fasciculus
MRI: Magnetic resonance imaging
MTG: Middle temporal gyrus
OR: Optic radiation
ROI: Region of interest
SLF: Superior longitudinal fasciculus
T1: Superior temporal gyrus
UF: Uncinate fasciculus
WM: White matter

From the [1]Skull Base and Cerebrovascular Laboratory and [2]Department of Neurological Surgery, University of California, San Francisco, San Francisco, California, USA; [3]Department of Neurological Surgery, Bellvitge University Hospital, L'Hospitalet de Llobregat, Barcelona, Spain; [4]Department of Neurological Surgery, Hospital Universitario Marqués de Valdecilla and Fundación Instituto de Investigación Marqués de Valdecilla, Santander, Spain; and [5]Department of Neurological Surgery, Barrow Neurological Institute, Phoenix, Arizona, USA

*To whom correspondence should be addressed: Ruth Lau, M.D.
[E-mail: ruth_lau_rodriguez@hotmail.com]*

*Citation: World Neurosurg. (2019) 128:e98-e106.
https://doi.org/10.1016/j.wneu.2019.04.034*

Journal homepage: www.journals.elsevier.com/world-neurosurgery

Available online: www.sciencedirect.com

Figure 1. Magnetic resonance images of a clinical case that could benefit from our proposed approach showing a lesion located in the left atrium in a T1-weighted sequence with gadolinium enhancement. (**A**) Coronal plane, (**B**) sagittal plane, and (**C**) axial plane.

critical neurovascular structures, and the close relationship of the atrium to crucial white matter (WM) pathways.[10,11]

Microsurgical approaches to the atrium have been broadly described in reported studies.[10-18] They can be divided into anterior (distal sylvian), posterior (transcortical, transcallosal, occipital, supracerebellar transtentorial), and lateral (transtemporal and subtemporal) approaches.[10-12] However, all have been associated with potentially severe complications. These have included auditory and visual deficits with the distal sylvian approach; injury to the optic radiations (ORs), aphasia, agnosia (dominant hemisphere) with the posterior transcortical approach; visual—verbal disconnection,[13] increased seizure risk,[14] and mutism[15] with the posterior transcallosal approach; venous infarction due to damage to the vein of Labbé with the subtemporal approach[10]; memory disturbance[12] in the occipital approach; and aphasia (dominant hemisphere) and quadrantanopsia[11] with the transtemporal approach.

The objective of the present study was to describe a novel surgical trajectory that has a safe entry point to access the atrium with minimal risk of transgressing critical cortical and subcortical structures. We tested the feasibility of an anterior endoscopic trans-middle temporal gyrus approach using both radiological data and, subsequently, surgical simulation. Additionally, WM dissections were performed to assess the extent of cortical transgression and damage to the WM tracts.

METHODS

Radiological Analysis

Ten de-identified patient magnetic resonance imaging (MRI) files (20 cerebral hemispheres) were used to delineate the optimal trajectory. The radiological images selected belonged to patients with no evidence of intraventricular pathology or indirect ventricular deformation. Using the Iplannet (BrainLab AG, Munich, Germany) software for cranial neuronavigation, we planned an anterior trans-middle temporal endoscopic trajectory to the atrium. The entry point into the cortex was defined in each hemisphere, with consideration of the location of the related WM tracts and cortical vessels. Thus, the surgical trajectory was aligned with the temporal horn of the lateral ventricle.

Virtual reconstruction of the WM tracts was performed using diffusion tensor imaging and 2 regions of interest (ROIs).[19,20] The fractional anisotropy in each voxel was set to an arbitrary threshold of 0.15.[19] For the inferior fronto-occipital fasciculus (IFOF), which courses from the ventral occipital lobe to the orbitofrontal cortex, 1 ROI was placed around the WM of the anterior floor of the external/extreme capsule and 1 ROI at the occipital lobe.[20] The uncinate fasciculus (UF) was defined as the area connecting the anterior temporal lobe with the medial and lateral orbitofrontal cortex.[21] The first ROI was placed in the anterior temporal lobe, and the second ROI at the extreme capsule. To perform the reconstruction of the segments of the superior longitudinal fasciculus (SLF), a single ROI was used, involving the half-moon shape in the most-dorsal part of the SLF. The lowest region was over the posterior temporal stem, and the medial border was identified lateral to the corona radiata. The precentral sulcus was defined as the anterior limit and the intraparietal sulcus as the posterior limit of the ROI.[20]

The inferior longitudinal fasciculus (ILF) connection between the occipital and temporal lobes was identified by placing the first ROI around the WM of the anterior temporal lobe and the second ROI on the lowest region of the occipital lobe.[20] The ORs were reconstructed using 2 ROIs. One ROI was located at the thalamus involving the lateral geniculate nucleus,[22] and the second ROI one was placed in the occipital lobe.

Surgical Simulation

The surgical simulation study was conducted using 13 cadaveric heads (24 specimens). Our customized embalming protocol[23] was used to prepare 10 cadaveric heads (19 specimens), and 3 cadaveric heads (5 specimens) were prepared using Klinger's standard embalming technique.[24] Klinger's embalming technique involves fixing the specimens in 10% formalin solution and storing them in a deep freezer at −15°C for 1 month. Before dissection, the specimens were thawed in cold water for 24 hours. Of these 5 specimens, 3 were specimens with calvaria and 2 were extracted brains. Our surgical approach was used for 3 cadaveric heads (6 specimens).

The feasibility of the proposed approach was examined using the remaining 13 specimens. A computed tomography (CT) scan was obtained for preoperative trajectory planning of each cadaveric head. Each specimen was positioned in a 3-pin head clamp (Mizuho Surgical Freedom Clamp [Mizuho Medical, Co., Ltd., Tokyo, Japan]) in a supine neutral position.

The specimens were registered using neuronavigation (Inav3 [Stryker, Kalamazoo, Michigan, USA]). The surgical trajectory was planned to implement the landmarks obtained in the radiological approach trajectory (Figure 2). A curvilinear skin incision was started at the tragus and turned anteriorly at the region of the superior temporal line to reach the midline just behind widow's peak (Figure 3). Using a subfascial dissection, the temporalis muscle was reflected and the zygomatic arch exposed. Next, a temporal craniotomy and orbitozygomatic osteotomy were performed.[25,26] Using a high-speed drill (5400-50 CORE [Stryker]), and the temporal craniotomy was extended inferiorly to the level of the middle fossa floor (Figure 4). On completion of the craniotomy, a cortical entry point was confirmed using the navigation system, and a 1-cm corticectomy was performed in the middle temporal gyrus, starting 1.5 cm posterior to the temporal pole. To reach the temporal horn from the corticectomy, we continued our transparenchymal dissection following the predefined trajectory.

Figure 3. Illustration of the curvilinear skin incision, which begins at the tragus and turns anteriorly at the region of the superior temporal line to reach the midline just behind widow's peak.

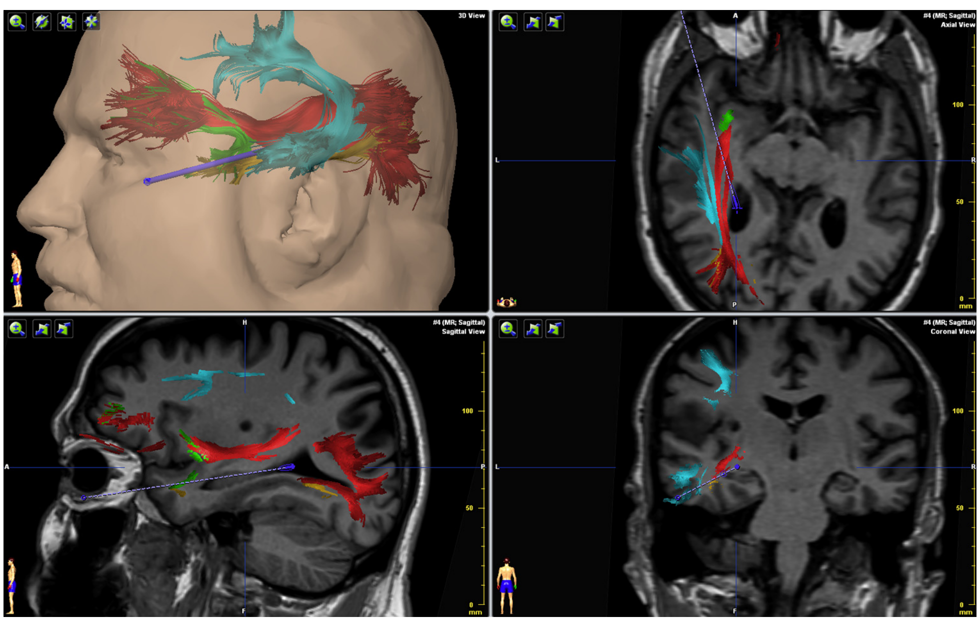

Figure 2. (**A**) Surgical planning of the intraventricular endoscopic approach using neuronavigation. The trajectory (*dark blue line*) is aligned with the atrium of the left ventricle. The relations of the uncinate fasciculus (*green*), inferior fronto-occipital fasciculus (*red*), superior longitudinal fasciculus (*blue*), and inferior longitudinal fasciculus (*orange*) to our trajectory are visualized.

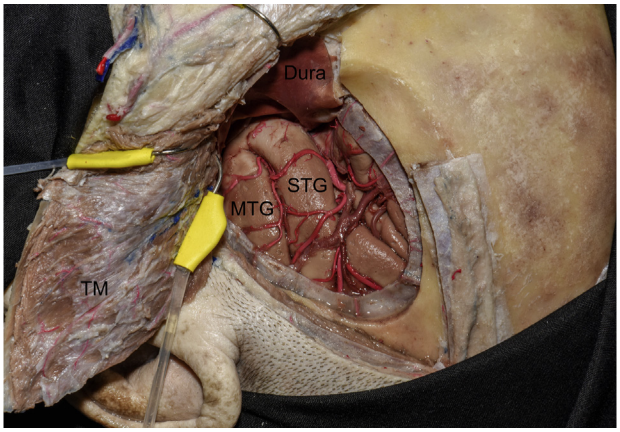

Figure 4. Photograph depicting the specimen after temporal craniotomy, orbitozygomatic osteotomy, and removal of the dura mater (Dura). PO, periorbita; STG, superior temporal gyrus; TM, temporalis muscle.

Once the temporal horn was reached with the endoscope (1488 HD System [Stryker]), the 0° lens was changed for a 30° lens (Figure 5), and a 14-gauge needle connected to an infusion system with water was placed in the frontal horn to simulate the presence of intraventricular cerebrospinal fluid during endoscopic navigation.

After identifying the atrium—cortical landmarks relevant to the ventricle location, the transparenchymal distance and trajectory lengths to the intraventricular landmarks were measured using the navigation system. The cortical landmarks we used were the temporal pole and the Sylvian anterior point. Thus, the following distances were measured: 1) distance from the temporal pole to the endoscope's entry point in the cortex measured over the temporal operculum; 2) distance from the endoscope's entry point to the Sylvian anterior point measured over the temporal operculum; 3) distance from the temporal pole to the endoscope's entry point measured over the superior temporal sulcus; and 4) the transparenchymal length as the distance from the endoscope's entry point to the entry point into the temporal horn. Furthermore, we measured the distance from the superior edge of the superior temporal gyrus (T1) to the inferior edge of the inferior temporal gyrus and the distance from the superior edge of T1 to the endoscope's entry point.

In all the specimens, we observed whether the angulation to access the temporal horn in the axial plane was related to the middle temporal gyrus, and whether in the sagittal plane, it was related to the Sylvian fissure. The following intraventricular landmarks were identified: 1) the inferior choroidal point (ICP), 2) choroid glomus, 3) collateral trigone, 4) calcar avis, and 5) medial atrial veins. We measured the distance from the endoscope's entry point in the cortex to each of these points to obtain the trajectory lengths. Finally, for each specimen, we recorded the most distal point we were able to reach with our tools.

WM Dissection

Five specimens were prepared using the standard Klinger method.[24] A preliminary assessment of the surgical trajectory related to the WM in the temporal pole was performed in 2 hemispheres. Subsequently, WM dissections (Figure 6A) of the anterior and long segments of the SLF, IFOF, UF (Figure 6B, C),[27-29] Meyer's loop,[30] ORs, and ILF (Figure 6D) were performed on the 3 specimens with calvaria in which the proposed surgical approach had been performed.[24] We recorded the presence of WM disruption of the dissected fascicles during the surgical simulation. Finally, the endoscopic transanterior middle temporal approach (ETMTA) was simulated using 1 specimen with WM dissection to analyze the subcortical integrity (Figure 7).

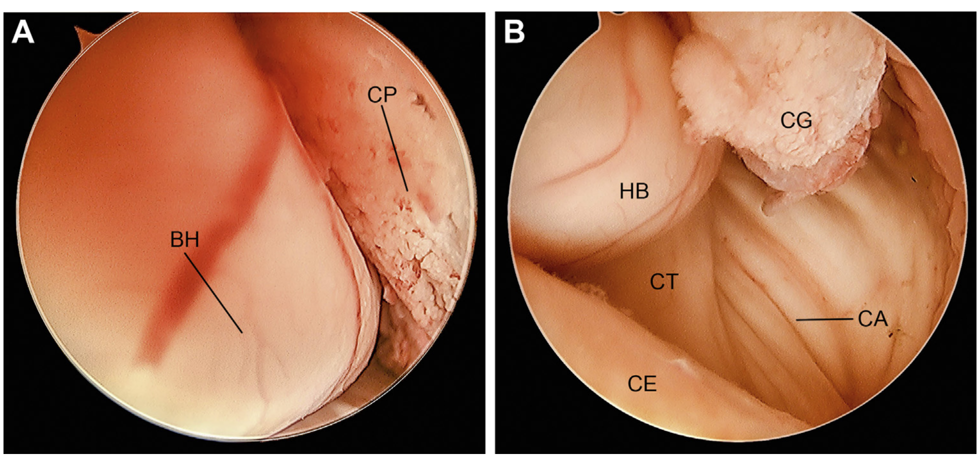

Figure 5. (**A**) Endoscopic intraventricular image using a 30° lens depicting the left temporal horn, body of the hippocampus (BH), and choroid plexus (CP). (**B**) Endoscopic intraventricular image showing the exposed atrium of the left temporal horn using a 30° lens. CA, calcar avis; CE, collateral eminence; CG, choroid glomus; CT, collateral trigone; HB, posterior part of the hippocampal body.

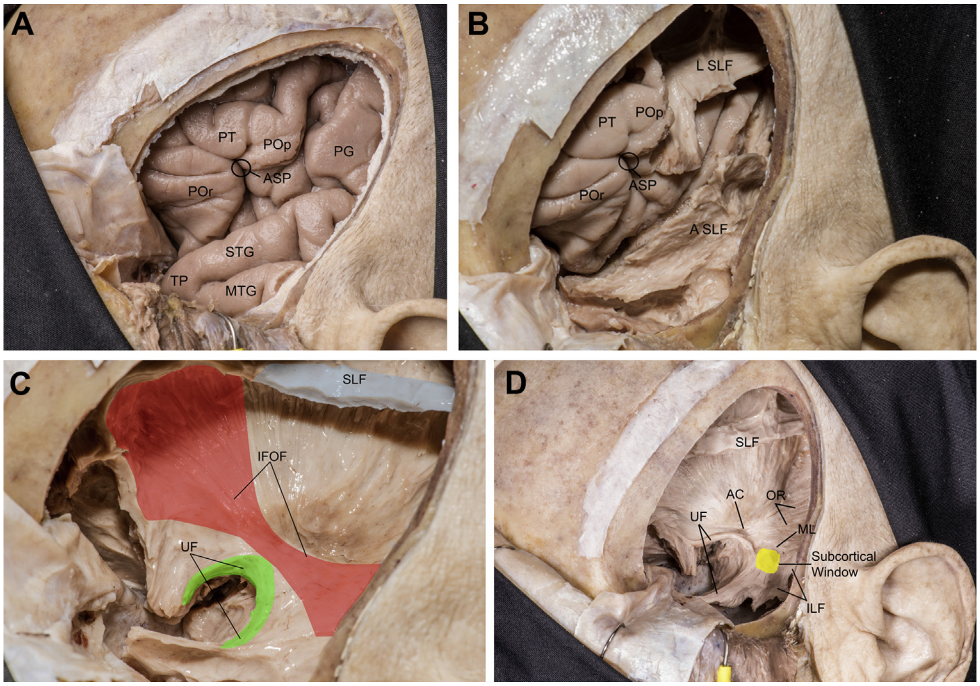

Figure 6. (**A**) Macroscopic view of the cortex in a Klinger-prepared specimen, depicting the main landmarks used for white matter (WM) dissection. (**B**) Depiction of a progressive WM dissection showing the anterior and longitudinal segments of the superior longitudinal fasciculus (SLF). The anterior segment of the SLF connects the posterior portion of the superior temporal gyrus with supramarginal gyrus and ventral portion of the precentral gyrus. The posterior portion conjoins the posterior portion of the middle and inferior temporal gyri, with the dorsal portion of precentral gyrus and pars opercularis. (**C**) Depiction of progressive WM dissection. After exposure of the insula and removal of the gray matter, extreme capsule, and claustrum—the uncinate fascicle (UF; *green*) at the limen of the insula and inferior fronto-occipital fascicle (IFOF; *red*) can both be visualized. *Blue* indicates the SLF. (**D**) Macroscopic image after extensive WM dissection. The IFOF has been removed. The UF, anterior commissure (AC), Meyer's loop (ML), optic radiations (OR), and inferior longitudinal fasciculus (ILF) are depicted. The proposed endoscopic trajectory through the subcortical window is marked (*yellow*). A SLF, anterior segment of SLF; ASP, anterior sylvian point; L SLF, long segment of the SLF; MTG, middle temporal gyrus; PG, precentral gyrus; POp, pars opercularis; POr, pars orbitalis; PT, pars triangularis; STG, superior temporal gyrus; TP, temporal pole.

RESULTS

Radiological Trajectory Planning

Our MRI study showed that the best entry angles to reach the atrium through a trans-middle temporal gyrus trajectory relative to the intercommissural line were $13.5° \pm 2.2°$ in the axial plane and $22.6° \pm 2.4°$ in the sagittal plane. Furthermore, we found that the best cortical entry point in the middle temporal gyrus was 19 ± 1.9 mm posterior to the temporal pole. These angles can be correlated to the Sylvian fissure in the sagittal plane and the temporal horn in the axial plane.

Cadaveric Simulation Study

The average transparenchymal distance from the corticectomy point to the ventricle was 24.5 ± 4.0 mm. The longest intraventricular measured trajectory was 46 ± 3.76 mm, corresponding to the calcar avis and medial atrial veins (Table 1).

The use of preoperative CT scans enabled accurate estimation of our surgical trajectory to the MRI planned trajectory. WM pathway dissection confirmed the integrity of the anterior segment of the SLF, IFOF, UF, ILF, and ORs. We found that the bundles in closest proximity to the endoscopic entry point to the ventricle were the posterior part of the UF and Meyer's loop—because our entry point was located posterior to the UF and anterior to the anterior wall of the temporal horn. Also, our strategized entry point into the ventricle is very close to the ILF. We created a trajectory that passes through a subcortical window, for which where the anterior wall is the UF, the superior walls are the IFOF ORs, and the inferior wall is the ILF (Figure 6C). For ease of reference, Figure 8 depicts all the referenced tracts divided just at the point at which the endoscope's trajectory crosses the WM through the subcortical window, avoiding the SLF, IFOF, UF, ILF, and ORs.

DISCUSSION

The ETMTA was successfully performed to reach the ventricular atrium in all cadaveric specimens in our study ($n = 24$). The eloquent WM tracts were not damaged using our proposed

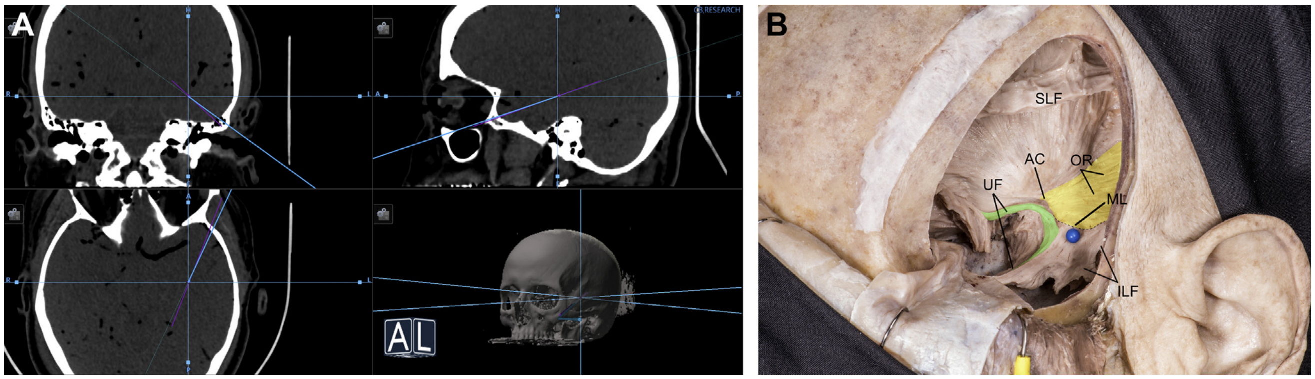

Figure 7. (**A**) Trajectory into the atrium as displayed on computed tomography-based neuronavigation system. (**B**) Photograph showing the entry point of the endoscope into the ventricular system (*blue pin*) posterior to the uncinate fasciculus (UF; *green*) and anterior to the optic radiations (OR; *yellow*) and Meyer's loop (ML). The inferior longitudinal fasciculus (ILF) is also shown. Our trajectory was confirmed by neuronavigation (*blue pin*). AC, anterior commissure; SLF, superior longitudinal fascicle (*blue*).

Table 1. Surgical Simulation Measurements of Relevant Landmarks and Distances

Measurement	Distance (mm)
Cortical points	
Related to temporal pole to endoscope entry point	
From temporal pole to endoscope entry point measured over temporal operculum	19 ± 1.9
From endoscope entry point to Sylvian anterior point measured over temporal operculum	16 ± 3.1
From temporal pole to endoscope entry point measured over superior temporal sulcus	17.1 ± 3.5
From endoscope entry point to entry point into ventricle (transparenchymal distance)	24.5 ± 4.1
Related to lateral surface of temporal lobe and endoscope entry point	
From superior part of T1 to edge of T3	40.5 ± 3.3
From superior part of T1 to endoscope entry point	16.1 ± 3.7
Intraventricular points	
From endoscope entry point into ventricle to intraventricular landmarks	
Endoscope entry point into ventricle to inferior choroidal point	9.3 ± 1.7
Endoscope entry point into ventricle to the choroid glomus	39.4 ± 3.9
Endoscope entry point into ventricle to posterior part of collateral trigone	44.3 ± 4.1
Endoscope entry point into ventricle to calcar avis	47.6 ± 2.7
Endoscope entry point into ventricle to medial atrial veins	46.1 ± 2

approach. In the present study, we have described a novel anterior endoscopic approach—through the most anterior part of the middle temporal gyrus—as a safe entry point to reach the ventricular atrium. Our proposed approach combines multiple neurosurgical subspecializations. We based our approach on the functional principles of neuro-oncology regarding the eloquent cortex and WM. We used a skull base approach—an orbitozygomatic craniotomy—to align the endoscope with the trajectory of the temporal horn to reach the atrium. It is necessary to remove the lateral wall of the orbit and the zygoma to provide enough maneuverability in the axial plane to enter the endoscope in the ventricular system through the most anterior part of the temporal horn. We also used neuroendoscopic techniques, which are essential to resecting tumors located in the atrium through a minimally invasive transparenchymal corridor. Finally, it is necessary to have functional endoscopic experience to perform our proposed approach successfully, because knowledge of the relevant widths of the intraventricular anatomy—which can be distorted by the presence of a lesion—are of great importance.

Procedure Trajectory

The procedure begins with a 1.0-cm corticectomy on the middle temporal gyrus, 1.5 cm posterior to the temporal pole. This trajectory avoids damaging the anterior edge of Meyer's loop, which is, on average, 31.4 mm from the temporal pole.[31,32] Numerous studies have identified a correlation between the extension of the lateral resection of the temporal lobe and the development of postoperative visual deficits. Anterior temporal lobe resection >31.3 mm from the pole of the temporal lobe has been associated with a 50% risk of visual field deficit.[33]

The location of the eloquent cortex has high interindividual variability; however, the anterior middle temporal gyrus is considered a place with a low probability of eloquence. Therefore, the approach we have presented might allow for a safer

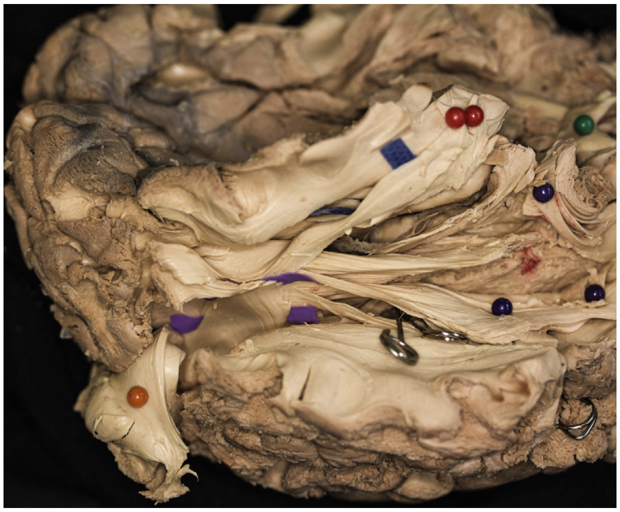

Figure 8. A Klinger-prepared left hemisphere after a cortex-sparing dissection. The uncinate fasciculus (*orange pin*), inferior fronto-occipital fascicle (*red pins*), and optic radiations (*blue pins*) are shown. The guide catheter marks the path of our trajectory into the temporal horn through a subcortical window, avoiding the uncinate fasciculus, inferior fronto-occipital fascicle, superior longitudinal fascicle (*green pin*), inferior longitudinal fascicle, Meyer's loop, and optic radiations.

corticectomy, because it traverses the anterior part of the middle temporal gyrus and avoiding critical regions.[34,35]

Relation to Existing Approaches

We consider that our approach provides better access to small to medium-size lesions located in the inferior part of the atrium with minimal distortion of the ipsilateral temporal horn. Compared with the distal sylvian approach, our approach might provide a safer corridor with less risk of damage to the auditory radiations.[10] In terms of functional outcomes, our approach carries a lower risk of aphasia and agnosia compared with the posterior transcortical approach.[36] Furthermore, the temporal posterior and inferior parietal approaches can damage several fascicles, including the SLF, ILF, middle longitudinal fasciculus, and ORs—described as the temporoparietal fiber intersection area.[37] This a critical crossroad that could produce multiple disconnection syndromes if violated, including aphasia, alexia, hemianopia, agraphia, and neglect.[38-40] Additionally, our newly proposed trajectory hypothetically avoids the risk of visual—verbal disconnection syndrome, 1 of the potential complications with the posterior transcallosal approach.[13]

With the ETMTA, we were able to achieve sound access and visualization of the collateral trigone, calcar avis, and medial atrial veins. Our trajectory also provides a better angle of view of the inferior part of the atrium compared with the occipital approach.[41] Furthermore, no retraction of the temporal lobe is performed, resulting in a decreased risk of Labbé damage and subsequent venous infarction.

Our results have demonstrated that our proposed approach provides a safe corridor between the anterior segment of the SLF, posterior part of the UF, inferior part of the IFOF, anterior part of the ORs, and the ILF, because these tracts are untouched. Having performed our approach on 19 specimens, our measurements were shown to be reliable in accurately coordinating the anatomical landmarks to access the temporal horn. Furthermore, the preoperative trajectory planned using MRI and CT was successfully correlated with the surgical simulation using neuronavigation. Therefore, preoperative planning using our proposed optimal trajectory can be used as a guide by neurosurgeons to access the temporal horn of the lateral ventricle. As an example, an imaging study of an atrial meningioma in the left hemisphere that could benefit from our proposed approach is shown in **Figure 1**.

Study Limitations

The objective of the present study was to demonstrate the anatomical feasibility and provide objective data that can serve as a reference for future research. Because our study used cadaveric simulations, it had several limitations. When performing the surgical approach, the effect of a lesion was missing owing to the absence of pathologic entities in the cadavers. Although our neurosurgical embalming procedure provided realistic brain retraction[23] and we re-created the cerebrospinal fluid flow dynamics, the presence of a lesion could alter these parameters.

As a purely surgical simulation study, clinical variables (e.g., length of hospital stay, morbidity, mortality), intraoperative events (e.g., extent of resection of the lesion, intraoperative bleeding), and postoperative deficits will need to be assessed in future clinical studies to determine the potential of this technique in treating clinical pathology.

Finally, given the interindividual anatomical variability, extensive neuroimaging must be performed before using this procedure to evaluate the local anatomy and any possible variations. Although we have provided specific landmarks that can be used to better understand the spatial relationship of the boundaries of the approach, laboratory training, the use of navigation systems, and careful patient selection should be considered before performing ETMTA in a clinical scenario. In our study, we used CT neuronavigation to reach the ventricular system with the endoscope. Also, the use of intraoperative ultrasonography can be a valuable technique for guidance in accessing the ventricular system. CT or MRI neuronavigation will provide the orientation in a fixed image. However, the use of ultrasonography allows for real-time images. Thus, fusing the information obtained from different modalities could help overcome their limitations. These imaging techniques could be especially valuable in locating an access point to the small temporal horns—which can be irrigated before cannulation with the endoscope. Furthermore, because we have described a new approach, we hope that the provided landmarks and measurements, in addition to neuronavigation and tractography, will help to overcome the limitations for application on a clinical case. Further clinical studies are necessary to gauge the safety and efficacy of our proposed technique.

CONCLUSION

We have presented a novel endoscopic approach that can potentially serve as an alternative method to reaching the ventricular atrium. We were able to reach the target area in all specimens, and we postulate that this approach will decrease the incidence of functional deficits resulting from transgression of the OR, IFOF, anterior segment of the SLF, ILF, and UF—persistent risks of standard techniques seeking to expose this region. The characteristics and landmarks reported in the present study could serve as a crucial addition to the armamentarium of any neurosurgeon performing such operations, and we highly recommend cadaveric simulation training for those interested.

ACKNOWLEDGMENTS

We would like to express our gratitude to the body donors and their families, who, through their altruism, contributed to making this project possible.

REFERENCES

1. Juretschke FR, Guresir E, Marquardt G, et al. Trigonal and peritrigonal lesions of the lateral ventricle-surgical considerations and outcome analysis of 20 patients. *Neurosurg Rev*. 2010;33: 457-464.

2. Nayar VV, DeMonte F, Yoshor D, Blacklock JB, Sawaya R. Surgical approaches to meningiomas of the lateral ventricles. *Clin Neurol Neurosurg*. 2010; 112:400-405.

3. Nakamura M, Roser F, Bundschuh O, Vorkapic P, Samii M. Intraventricular meningiomas: a review of 16 cases with reference to the literature. *Surg Neurol*. 2003;59:491-503 [discussion: 503, 494].

4. Gokalp HZ, Yuceer N, Arasil E, et al. Tumours of the lateral ventricle: a retrospective review of 112 cases operated upon 1970-1997. *Neurosurg Rev*. 1998;21:126-137.

5. Smith AB, Smirniotopoulos JG, Horkanyne-Szakaly I. From the radiologic pathology archives: intraventricular neoplasms: radiologic-pathologic correlation. *Radiographics*. 2013;33:21-43.

6. Louis DN, Perry A, Reifenberger G, et al. The 2016 World Health Organization classification of tumors of the central nervous system: a summary. *Acta Neuropathol*. 2016;131:803-820.

7. Silver AJ, Ganti SR, Hilal SK. Computed tomography of tumors involving the atria of the lateral ventricles. *Radiology*. 1982;145:71-78.

8. Cecchi PC, Billio A, Colombetti V, Rizzo P, Ricci UM, Schwarz A. Primary high-grade B-cell lymphoma of the choroid plexus. *Clin Neurol Neurosurg*. 2008;110:75-79.

9. Stavrinou LC, Stranjalis G, Flaskas T, Sakas DE. Trigonal cavernous angioma: a short illustrated review. *Acta Neurochir*. 2009;151:1517-1520.

10. Kawashima M, Li X, Rhoton AL Jr, Ulm AJ, Oka H, Fujii K. Surgical approaches to the atrium of the lateral ventricle: microsurgical anatomy. *Surg Neurol*. 2006;65:436-445.

11. Gungor A, Baydin S, Middlebrooks EH, Tanriover N, Isler C, Rhoton AL Jr. The white matter tracts of the cerebrum in ventricular surgery and hydrocephalus. *J Neurosurg*. 2017;126: 945-971.

12. Jeelani Y, Gokoglu A, Anor T, Al-Mefty O, Cohen AR. Transtentorial transcollateral sulcus approach to the ventricular atrium: an endoscope-assisted anatomical study. *J Neurosurg*. 2017;126: 1246-1252.

13. Moftakhar R, Izci Y, Baskaya MK. Microsurgical anatomy of the supracerebellar transtentorial approach to the posterior mediobasal temporal region: technical considerations with a case illustration. *Neurosurgery*. 2008;62(suppl 1):1-7 [discussion: 7-8].

14. Nagib MG, O'Fallon MT. Lateral ventricle choroid plexus papilloma in childhood: management and complications. *Surg Neurol*. 2000;54:366-372.

15. Weil AG, Middleton AL, Niazi TN, Ragheb J, Bhatia S. The supracerebellar-transtentorial approach to posteromedial temporal lesions in children with refractory epilepsy. *J Neurosurg Pediatr*. 2015;15:45-54.

16. Wang S, Salma A, Ammirati M. Posterior interhemispheric transfalx transprecuneus approach to the atrium of the lateral ventricle: a cadaveric study. *J Neurosurg*. 2010;113:949-954.

17. Zhu W, Xie T, Zhang X, et al. A solution to meningiomas at the trigone of the lateral ventricle using a contralateral transfalcine approach. *World Neurosurg*. 2013;80:167-172.

18. Wang X, Yang L, Zhang H, Yan Z, She L. Microsurgical and endoscopic posterior transcortical keyhole approach to the atrium of the lateral ventricle: a cadaveric study. *J Neurol Surg A Cent Eur Neurosurg*. 2015;76:261-267.

19. Catani M, Howard RJ, Pajevic S, Jones DK. Virtual in vivo interactive dissection of white matter fasciculi in the human brain. *Neuroimage*. 2002;17: 77-94.

20. Catani M, Thiebaut de Schotten M. A diffusion tensor imaging tractography atlas for virtual in vivo dissections. *Cortex*. 2008;44:1105-1132.

21. Duffau H, Gatignol P, Mandonnet E, Peruzzi P, Tzourio-Mazoyer N, Capelle L. New insights into the anatomo-functional connectivity of the semantic system: a study using cortico-subcortical electrostimulations. *Brain*. 2005;128(Pt 4):797-810.

22. Wu W, Rigolo L, O'Donnell LJ, Norton I, Shriver S, Golby AJ. Visual pathway study using in vivo diffusion tensor imaging tractography to complement classic anatomy. *Neurosurgery*. 2012; 70(1 suppl operative):145-156 [discussion: 156].

23. Benet A, Rincon-Torroella J, Lawton MT, Gonzalez Sanchez JJ. Novel embalming solution for neurosurgical simulation in cadavers. *J Neurosurg*. 2014;120:1229-1237.

24. Koutsarnakis C, Liakos F, Kalyvas AV, Sakas DE, Stranjalis G. A laboratory manual for stepwise cerebral white matter fiber dissection. *World Neurosurg*. 2015;84:483-493.

25. Poblete T, Jiang X, Komune N, Matsushima K, Rhoton AL Jr. Preservation of the nerves to the frontalis muscle during pterional craniotomy. *J Neurosurg*. 2015;122:1274-1282.

26. Tayebi Meybodi A, Lawton MT, Yousef S, Sanchez JJG, Benet A. Preserving the facial nerve during orbitozygomatic craniotomy: surgical anatomy assessment and stepwise illustration. *World Neurosurg*. 2017;105:359-368.

27. Martino J, De Witt Hamer PC, Berger MS, et al. Analysis of the subcomponents and cortical terminations of the perisylvian superior longitudinal fasciculus: a fiber dissection and DTI tractography study. *Brain Struct Funct*. 2013;218:105-121.

28. Martino J, De Lucas EM. Subcortical anatomy of the lateral association fascicles of the brain: a review. *Clin Anat*. 2014;27:563-569.

29. Martino J, Brogna C, Robles SG, Vergani F, Duffau H. Anatomic dissection of the inferior fronto-occipital fasciculus revisited in the lights of brain stimulation data. *Cortex*. 2010;46:691-699.

30. Goga C, Ture U. The anatomy of Meyer's loop revisited: changing the anatomical paradigm of the temporal loop based on evidence from fiber microdissection. *J Neurosurg*. 2015;122:1253-1262.

31. Choi C, Rubino PA, Fernandez-Miranda JC, Abe H, Rhoton AL Jr. Meyer's loop and the optic radiations in the transsylvian approach to the mediobasal temporal lobe. *Neurosurgery*. 2006; 59(suppl 2):ONS228-ONS235 [discussion: ONS235, ONS226].

32. Fernandez-Miranda JC, Rhoton AL Jr, Alvarez-Linera J, Kakizawa Y, Choi C, de Oliveira EP.

Three-dimensional microsurgical and tractographic anatomy of the white matter of the human brain. *Neurosurgery*. 2008;62(suppl 3):989-1026 [discussion: 1026-1028].

33. Krolak-Salmon P, Guenot M, Tiliket C, et al. Anatomy of optic nerve radiations as assessed by static perimetry and MRI after tailored temporal lobectomy. *Br J Ophthalmol*. 2000;84:884-889.

34. Duffau H. A two-level model of interindividual anatomo-functional variability of the brain and its implications for neurosurgery. *Cortex*. 2017;86: 303-313.

35. Ojemann G, Ojemann J, Lettich E, Berger M. Cortical language localization in left, dominant hemisphere: an electrical stimulation mapping investigation in 117 patients. *J Neurosurg*. 2008;108: 411-421.

36. Kawashima M, Rhoton AL Jr, Matsushima T. Comparison of posterior approaches to the posterior incisural space: microsurgical anatomy and proposal of a new method, the occipital bi-transtentorial/falcine approach. *Neurosurgery*. 2002;51: 1208-1220 [discussion: 1220, 1201].

37. Martino J, da Silva-Freitas R, Caballero H, Marco de Lucas E, Garcia-Porrero JA, Vazquez-Barquero A. Fiber dissection and diffusion tensor imaging tractography study of the temporoparietal fiber intersection area. *Neurosurgery*. 2013;72(1 suppl operative):87-97 [discussion: 97, 88].

38. Doricchi F, Tomaiuolo F. The anatomy of neglect without hemianopia: a key role for parietal-frontal disconnection? *Neuroreport*. 2003;14:2239-2243.

39. Sakurai Y, Asami M, Mannen T. Alexia and agraphia with lesions of the angular and supramarginal gyri: evidence for the disruption of sequential processing. *J Neurol Sci*. 2010;288:25-33.

40. Ihori N, Kawamura M, Araki S, Kawachi J. Kinesthetic alexia due to left parietal lobe lesions. *Eur Neurol*. 2002;48:87-96.

41. Sanchez JJ, Rincon-Torroella J, Prats-Galino A, et al. New endoscopic route to the temporal horn of the lateral ventricle: surgical simulation and morphometric assessment. *J Neurosurg*. 2014;121: 751-759.

Conflict of interest statement: The authors declare that the article content was composed in the absence of any commercial or financial relationships that could be construed as a potential conflict of interest.

Received 13 December 2018; accepted 3 April 2019

Citation: World Neurosurg. (2019) 128:e98-e106.
https://doi.org/10.1016/j.wneu.2019.04.034

Journal homepage: ***www.journals.elsevier.com/world-neurosurgery***

Available online: ***www.sciencedirect.com***